Aalborg Universitet

AALBORG UNIVERSITY
DENMARK

Development and Experimental Validation of an Ultra-wideband Channel Sounder

Fan, Wei; Mbugua, Allan Wainaina; Cai, Xuesong; Olesen, Kim

Development and Experimental Validation of an Ultra-wideband Channel Sounder

Wei Fan, Allan Wainaina Mbugua, Xuesong Cai, Kim Olesen

Antennas, Propagation and Millimeter-wave Systems (APMS) Section, Department of Electronic Systems, Aalborg University, 9000, Aalborg, Denmark

Abstract—Vector network analyzer (VNA) has been extensively utilized for radio channel sounding purposes. Due to its slow channel sounding speed, it has been mainly used for channel measurements in static propagation scenarios. The main limitation with VNA based channel sounder is its small measurement range, due to signal attenuation in the coaxial cable setup. Employing radio over fiber (RoF) can effectively eliminate the cable loss and hence enables the VNA for long range channel sounding. However, optical cables are sensitive to phase changes in optical cables in practical usage scenarios. In this paper, two phase correction strategies, i.e. two-branch scheme and bi-directional scheme, are discussed and experimentally validated to remove the random phase change in the cable. The bi-directional scheme is shown to be highly effective in removing the phase change in the measurements. The virtual array VNA channel sounder employing RoF technique and phase correction scheme is highly attractive, since it supports channel sounding with arbitrary frequency carrier setting, ultra-wideband, large-scale (virtual) antenna settings with a large measurement range.

I. INTRODUCTION

Understanding of how radio signal propagates in realistic environments is key to the design and development of wireless systems [1], [2]. Fundamentally, wireless system designs begin with the understanding of deployment environment, where reliable measurements of channels (i.e. channel sounding) are required. Both modeling and characterization of the radio channel start with reliable measurements of channels in the deployment scenarios. The fifth generation (5G) new radio (NR) will explore many advanced features, e.g. large-scale antenna configuration, ultra-wide bandwidth, millimeter wave frequencies, etc. However, these new features have posed huge challenges on channel sounders. To support for 5G NR channel modeling work, the ideal channel sounder should be designed to meet several objectives, for example [1]:

- Ultra-wide-band system bandwidth. 5G NR systems operating at millimeter wave bands rely on the large available bandwidth to achieve high data-rate. Further, a large bandwidth is desirable to obtain a high delay resolution in channel sounding.
- Flexible frequency setting. Various frequency bands up to 100 GHz have been proposed for 5G NR. It is difficult to assess frequency bands and required bandwidths for 5G NR deployment at current stage. Further, for system design and development, it is important to understand whether channel characteristics at various frequency bands differ.

- High measurement speed. Channel sounding speed should be sufficiently high so that the channel measurements of all links are performed within the channel coherence time.
- Channel sounding with massive antenna elements. Massive multiple-input multiple-output (MIMO) channel sounding with real and virtual large-scale antenna arrays have been reported in the literature.
- Long measurement distance between the transmitter (Tx) and receiver (Rx). Channel sounder should support for measurement ranges in various deployment scenarios, e.g. indoor, outdoor, etc.
- High dynamic range. High dynamic range is desirable for channel sounding in order to detect weak paths as well as dominant paths in the radio channels.

Channel sounding techniques can be grouped into two categories, i.e. the time-domain sounding techniques, and the frequency-domain sounding techniques. The time-domain technique offers high measurement speed, thereby making it suitable for sounding dynamic radio channels. However, it typically has a specific measurement setting, e.g. fixed carrier frequency and bandwidth, and limited dynamic range. The frequency-domain channel sounders, e.g. vector network analyzer (VNA) based, are more flexible and offers high dynamic range. Measurement frequency and bandwidth can be set to arbitrary configurations supported by the VNA systems. The disadvantage of the VNA based channel sounder is its relatively slow measurement speed in frequency sweeping, which limit its application scenario mainly to static indoor scenarios [3]–[6].

Channel sounding systems with real or virtual large-scale antenna arrays have been reported in the literature. Real-array channel sounder systems (either with parallel or switched structure) are often capable of capturing dynamic channel characteristics. However, real large-scale antenna channel sounder are often cost-prohibitive and complicated [1]. Virtual large-scale array is typically formed via mechanically re-positioning a single antenna element or sub-array system at predefined locations. The virtual large-scale array system is attractive and widely adopted, due to its simplicity, low cost and flexibility. One drawback is that it can only be applied in static environments, since it is assumed that channel profiles remain static during channel sounding at all element locations (i.e. array elements in the virtual array) [3]–[6].

Virtual array VNA based channel sounder is an attractive solution for channel sounding in static propagation scenarios. It allows flexible bandwidth and frequency settings and offers

high dynamic range. Further, channel sounding with massive antenna elements can be mimicked in a cost-effective and flexible way with the virtual array concept. The measurement range (i.e. distance between Tx and Rx) is the major limitation for VNA based system. A cable between Tx and Rx is required in the VNA setup, both as signal carrier and also for synchronization purpose. However, signal power attenuates along the co-axial cable. The co-axial cable attenuation, typically defined in terms of decibels per unit length at a given frequency, effectively reduces the system dynamic range. As a result, the measurement range is limited, especially when the measurement frequency is high. Two solutions have been proposed in the literature to address this issue. The first one utilizes frequency mixers to down-convert signals to a lower frequency on the co-axial cable to reduce cable loss, thereby effectively increasing the measurement range. The second one replaces co-axial cable with radio-over-fiber (RoF) techniques, due to negligible transmission loss on optical cables. This technique is an ideal solution for long-range channel sounding with VNA systems. However, the signal phase is highly sensitive to mechanical stress (e.g. cable bending) and thermal on optical cables, which prevents its usage for virtual array channel sounding. Advanced signal processing techniques in massive MIMO systems (e.g. channel parameter estimation) rely heavily on accurate phase information accuracy. Consequently, VNA based channel sounders employing RoF technologies have been mainly used with rotational horn antennas, where coherent phase information among virtual array elements is typically not utilized.

In this paper, we develop a VNA channel sounder based on RoF technology with a phase correction schemes. The developed channel sounder supports massive virtual array measurement with high dynamic range, arbitrary frequency bandwidth and carrier frequency setting and long measurement range. In Section II, we demonstrate the RoF setup and phase issues related to the setup for virtual array measurements. We present and compare three alternative phase correction schemes for the RoF solution in Section III. In Section IV, the proposed channel sounder is experimentally validated in anechoic chamber, and Section V concludes the paper.

II. RADIO-OVER-FIBER BASED CHANNEL SOUNDER

A. Basic configuration

VNA is an intrinsic channel sounder, where the radio channel frequency response $h_{12}(f)$ can be measured in the $S_{21}(f)$ in the S parameter set as:

$$S_{21}(f) = h_c(f)h_{12}(f)$$

$h_c(f)$ is the frequency response of the cables and optical transmitter (Tx) and receiver (Rx). $h_{12}(f)$ includes the effect of the Tx antennas and Rx antennas and the propagation channel frequency response. A back-to-back connection is shown in Fig. 1 (top).

B. Problem statement

Employing RoF technique can significantly extend the measurement range, as explained earlier. However, the main
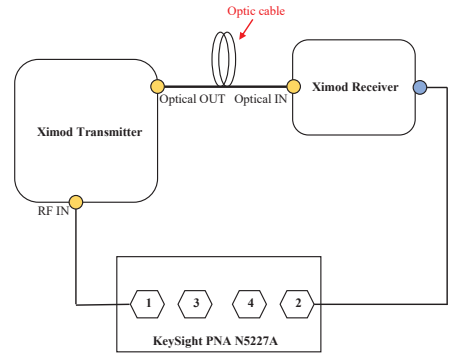

Figure 1. Back-to-back configuration for the VNA system.

problem with the basic configuration is the phase change in the system components, mainly in the optical cable. Phases are highly sensitive to the temperature in the environment. For VNA based measurement, the measurement time can be long, especially when a large number of measurements are needed (e.g. for the virtual array channel sounding). Another main contributor for phase instability is the cable bending. Cable bending is inevitable in practical usage, which can cause significantly phase change, depending on the bending radius.

A simple measurement to investigate the cable bending effect on the phase change was performed, where the basic back-to-back configuration is adopted. The impact of cable bending on the phase change can be clearly observed in Fig. 2. In the results, the phase change is normalized to the phase response with 60 cm bending diameter. The slopes of the phase response with different cable bending diameters are different, indicating different electrical lengths with cable bending. The amplitude response is not noticeably affected by the cable bending from frequency up to 30 GHz, with a variation up to 0.5 dB. From 30 GHz to 50 GHz, an amplitude variation up to ±1.5dB is observed. The phase change over time was also investigated. The phase response was recorded at 26.5 GHz to 30 GHz continuously for a period of 17 hours, and data is saved every 15 minutes.

The phase change can be up to ±30 degrees within the 17 hours. The system frequency response $h_c(f)$ can be compensated in a back-to-back measurement. Introducing a frequency dependent term $\triangledown h(f)$ to denote the phase change in the system, we have

$$S_{21}(f) = \triangledown h(f)h_{12}(f) \tag{1}$$

Note that the term $\triangledown h(f)$ is typically random and not known beforehand, which means it would be difficult to calibrate it out directly. The random term $\triangledown h(f)$ will be embedded in the results, which will be problematic for phase-critical applications, e.g. channel sounding.

III. PHASE COMPENSATION TECHNIQUES

As demonstrated earlier, phase change due to cable bending (mechanical stress) and temperature (signal drifting) can be significant. In this section, two schemes to correct the phase change are proposed and discussed.
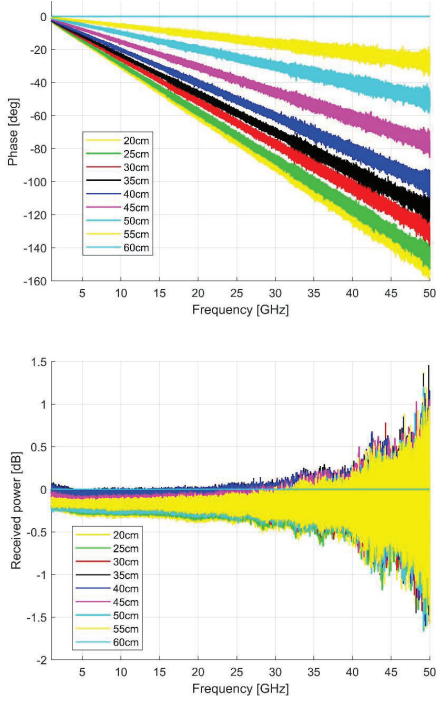
Figure 2. Phase (top) and amplitude (below) response over frequency band with different cable bending diameters.
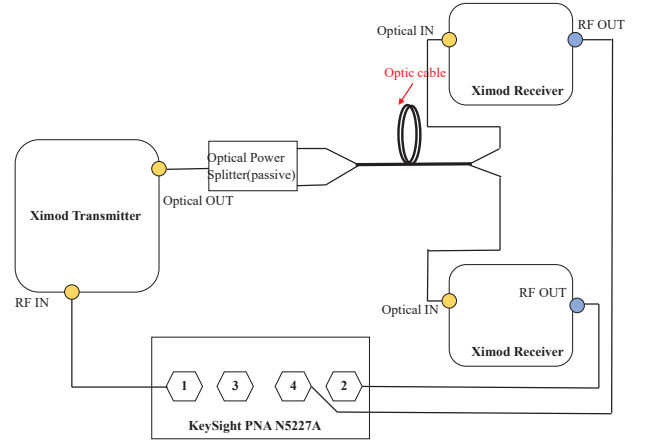

Figure 3. Two branch transmission scheme for phase tracking and correction.
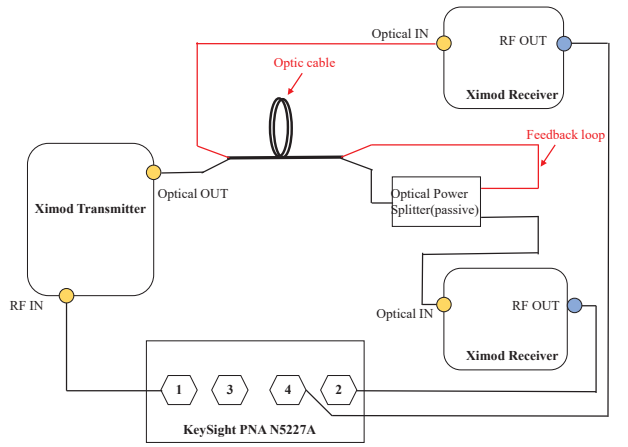
Figure 4. Bi-directional transmission scheme for phase tracking and correction.

A. Two-branch scheme

One straightforward way to track and correct phase change is to adopt a two-branch scheme utilizing an optical splitter, as illustrated in Fig. 3. We have

$$S_{21}(f) = h_1(f) \bigtriangledown h_1(f) h_{12}(f) \tag{2}$$

$$S_{41}(f) = h_2(f) \bigtriangledown h_2(f) \tag{3}$$

where $h_1(f)$ and $h_2(f)$ are the system frequency response of link 1 and link 2, respectively. $\bigtriangledown h_1(f)$ and $\bigtriangledown h_2(f)$ denote the random frequency response in link 1 and link 2, respectively. $h_1(f)$ and $h_2(f)$ can be easily calibrated out ($h_1(f) = h_2(f) = 1$) in the back-to-back measurement. Therefore, if we have two links with identical cable length and movement, we can assume same phase change in link 1 and link 2 (i.e. $\bigtriangledown h_1(f) = \bigtriangledown h_2(f)$). After back-to-back calibration, we have:

$$h_{12}(f) = \frac{S_{21}(f)}{S_{41}(f)} \tag{4}$$

B. Bi-directional transmission scheme

A bi-directional transmission scheme can be achieved utilizing optical circulators and optical power splitter, as illustrated in Fig. 4. For the forward link, we have

$$S_{21}(f) = h_{FW}(f) \bigtriangledown h(f) h_{12}(f) \tag{5}$$

where $h_{FW}(f)$ denotes the frequency response of the forward link. For the feedback link, we have

$$S_{41}(f) = h_{FB}(f) \bigtriangledown h(f)^2 \tag{6}$$

where $h_{FW}(f)$ denotes the frequency response of the feedback link. We have $\bigtriangledown h(f)$ in the forward link and $\bigtriangledown h(f)^2$ in the feedback link since the signal travels once in the forward link and twice in the backward link. $h_{FW}(f)$ and $h_{FB}(f)$ can be again calibrated out in the back-to-back measurements.

Adopting the bi-directional transmission scheme, the radio channel frequency response can be measured as:

$$h_{12}(f) = \frac{S_{21}(f)}{\sqrt{S_{41}(f)}} \tag{7}$$

IV. EXPERIMENTAL VALIDATIONS

The two proposed scheme was experimentally validated in back-to-back measurements. Note that the optical cable was put on a turntable during the measurement. The phase response was recorded at various rotation angles of the turntable.
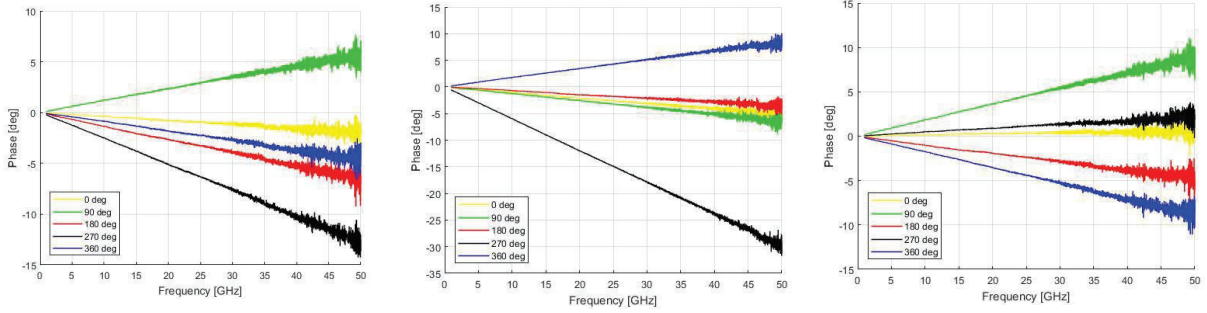
Figure 5. The phase change of the link 1 (left), link 2 (middle) and corrected result (right) with the two branch sheme.

A. Back to back measurement

The phase changes of link 1 and link 2 from 1 GHz to 50 GHz are shown in Fig. 5 (left) and Fig. 5 (middle), respectively. As we can see, the phase change in link 2 approximately follows that of link 1 over the frequency band for all cable bending diameters. Adopting Eq. (5), the corrected phase response using the two-branch scheme is shown in Fig. 5 (right). The two-branch scheme can mitigate the phase change introduced by the cable bending. However, phase change still exists with the phase correction scheme, up to 10° phase variation from 1 GHz to 50 GHz due to the fact that the cable movement at the two branches are not exactly identical (i.e. $\triangledown h_1(f) \neq \triangledown h_2(f)$).

The phase changes of the forward link and feedback link from 1 GHz to 50 GHz are shown in Fig. 6 (left) and Fig. Fig. 6 (middle) with the bi-directional transmission scheme, respectively. The measured phase response over frequency of the feedback link is always approximately twice that of the forward link, indicating the effectiveness of the bi-directional transmission scheme. The corrected phase response, adopting Eq. (7) is shown in Fig. 6 (right), where an phase error of up to ± 2 degrees from 1 GHz to 30 GHz can be observed. The bi-directional transmission scheme outperforms the two branch scheme due to the fact that same cable is utilized. Therefore, phase change in the cable can be accurately recorded and corrected.

B. Anechoic chamber measurements

To evaluate the over-the-air performance of the measurement system, a validation measurement in an anechoic chamber as illustrated in Fig. 7 was conducted. Two antennas with omni-directional radiation patterns in azimuth were exploited in Tx and Rx sides, respectively. A virtual 30×30 uniform rectangular array (URA) was formed by moving the Tx antenna to pre-defined locations as illustrated in Fig. 8, where the inter-element spacing was 0.4 wavelength at 30 GHz. The Tx antenna was fixed at the same height to the Rx antenna during the measurement. The propagation channel in the anechoic chamber was recorded by sweeping the frequency band from 26.5 GHz to 30 GHz with 6000 frequency points.

It can be expected that if the propagation channel only consists of line-of-sight (LoS) path, the phases of the channel

coefficients across the 900 different Rx locations at a fixed frequency point can be directly obtained from the measurement data. Meanwhile, the correspondingly theoretical values can be easily calculated according to the geometry as illustrated in Fig. 8. However, ideal propagation with only LoS path does not exist due to the imperfection of the chamber and the existence of measurement equipment. Benefiting from the ultra-wide bandwidth, the Space-Alternating Generalized Expectation-maximization (SAGE) algorithm [7] is alternatively exploited to extract the LoS paths at individual Rx locations. Fig. 9 illustrates the comparison between the empirical LoS phase shifts and the theoretical LoS phase shifts at 30 GHz across the array. It can be observed that empirical and theoretical values match well. The deviation is most likely introduced by errors in the geometrical alignment of the antennas.
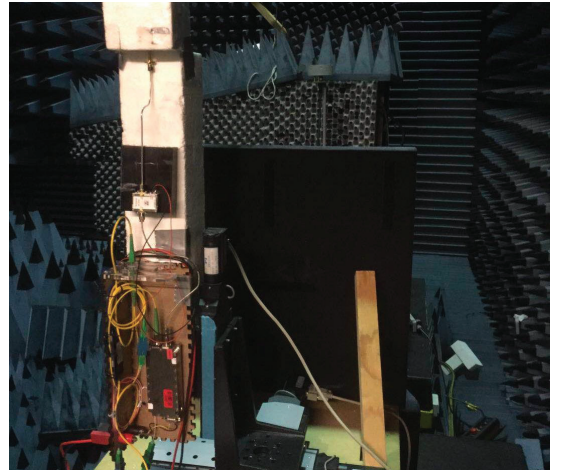

Figure 7. A photo of the measurement setup in the anechoic chamber.

V. CONCLUSION

In this paper, two phase correction schemes are proposed and experimentally validated. The bi-directional transmission, which is achieved via optical circulators and splitters, is shown to be highly effective in correcting the phase changes in the optical cables. The two branch scheme, realized via optical splitters, though shown to work in some extent, might
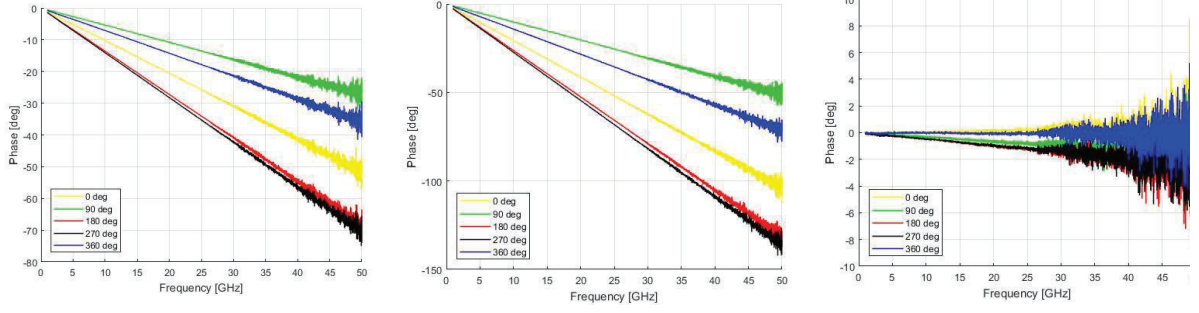
Figure 6. The phase change of the forward link (left), feedback link (middle) and corrected result (right) with the bi-directional sheme.
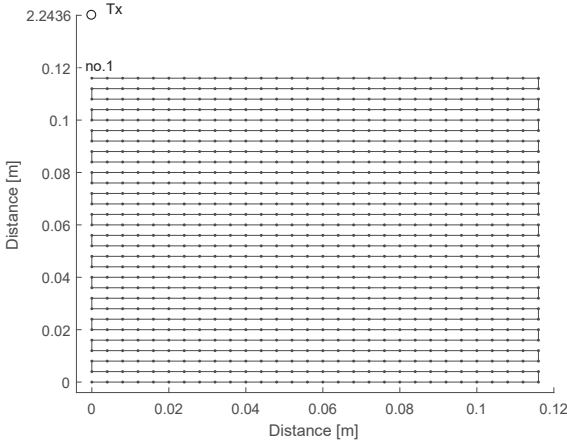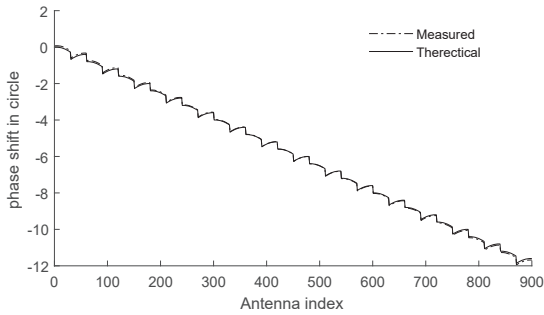

Figure 8. Virtual array element trajectory.

Figure 9. Measured and theorectical phase across antenna elements for the LOS component.

fail to provide accurate phase correction results, due to the difference between two branches in practice. The virtual array channel sounder employing RoF techniques and bi-directional transmission phase correction scheme is highly attractive for 5G propagation research, due to its capability of providing ultra-wideband long range channel sounding with arbirtrary frequency setting and high dynamic range.

ACKNOWLEDGMENT

REFERENCES

[1] J. Nielsen, W. Fan, P. Eggers, and G. Pedersen, "A channel sounder for massive MIMO and mmwave channels," *IEEE Communications Magazine*, 8 2018.

[2] G. R. MacCartney and T. S. Rappaport, "A flexible millimeter-wave channel sounder with absolute timing," *IEEE Journal on Selected Areas in Communications*, vol. 35, no. 6, pp. 1402–1418, June 2017.

[3] Y. Ji, W. Fan, and G. F. Pedersen, "Channel characterization for wideband large-scale antenna systems based on a low-complexity maximum likelihood estimator," *IEEE Transactions on Wireless Communications*, vol. 17, no. 9, pp. 6018–6028, Sept 2018.

[4] W. Fan, I. Carton, J. Ø. Nielsen, K. Olesen, and G. F. Pedersen, "Measured wideband characteristics of indoor channels at centimetric and millimetric bands," *EURASIP Journal on Wireless Communications and Networking*, vol. 2016, no. 1, p. 58, Feb 2016.

[5] J. Medbo, H. Asplund, and J. . Berg, "60 GHz channel directional characterization using extreme size virtual antenna array," in *IEEE 26th Annual International Symposium on Personal, Indoor, and Mobile Radio Communications (PIMRC)*, Aug 2015, pp. 176–180.

[6] A. W. Mbugua, W. Fan, Y. Ji, and G. F. Pedersen, "Millimeter wave multi-user performance evaluation based on measured channels with virtual antenna array channel sounder," *IEEE Access*, vol. 6, pp. 12 318–12 326, 2018.

[7] B. H. Fleury, M. Tschudin, R. Heddergott, D. Dahlhaus, and K. I. Pedersen, "Channel parameter estimation in mobile radio environments using the SAGE algorithm," *IEEE Journal on Selected Areas in Communications*, vol. 17, no. 3, pp. 434–450, Mar 1999.